Production of green hydrogen from sewage sludge / algae in agriculture diesel engine: Performance Evaluation

Venkatesh Rathinavelu [a], Arul Kulandaivel [b], Arvind Kumar Pandey [c], Rahul Bhatt [d], Melvin Victor De Poures [a], Ismail Hossain [e], Asiful Hossain Seikh [f], Amjad Iqbal [g], P. Murugan [h],*

[a] Department of Mechanical Engineering, Saveetha School of Engineering, Saveetha Institute of Medical and Technical Sciences (SIMATS), Chennai 602105, Tamilnadu, India
[b] Department of Mechanical Engineering, Agni College of Technology, Chennai, 600130, Tamilnadu, India
[c] Department of Computer Science, ARKA JAIN University, Jamshedpur, 831001, Jharkhand, India
[d] Department of Computer Science and Engineering, Dev Bhoomi Uttarakhand University, Dehradun, Uttarakhand, India
[e] School of Natural Sciences and Mathematics, Ural Federal University, Yekaterinburg, 620000, Russia
[f] Mechanical Engineering Department, College of Engineering, King Saud University, Riyadh 11421, Saudi Arabia
[g] Department of Materials Technologies, Faculty of Materials Engineering, Silesian University of Technology, 44-100, Gliwice, Poland
[h] Department of Mechanical Engineering, Jimma Institute of Technology, JIMMA University, Ethiopia

ARTICLE INFO

ABSTRACT

Alternative fuel opportunities can satisfy energy security and reduce carbon emissions. In this regard, the hydrogen fuel is derived from the source of environmental pollutants like sewage and algae wastewater through hydrothermal gasification technique using a KOH catalyst with varied gasification process parameters of duration and temperature of 6–30 min and 500-800 °C. The novelty of the work is to identify the optimum gasification process parameter for obtaining the maximum hydrogen yield using a KOH catalyst as an alternative fuel for agricultural engine applications. Influences of gasification processing time and temperature on H_2 selectivity, Carbon gasification efficiency (CE), Lower heating value (LHV), Hydrogen yield potential (HYP), and gasification efficiency (GE) were studied. Its results showed that the gasifier operated at 800 °C for 30 min, offering maximum hydrogen yield (26 mol/kg) and gasification efficiency (58 %). The synthesized H_2 was an alternative fuel blended with diesel fuel/TiO_2 nanoparticles. It was experimentally studied using an internal combustion engine. Influences of H_2 on engine performance, like brake-specific fuel consumption, brake thermal efficiency and emission performances, were measured and compared with diesel fuel. The results showed that DH20T has the least (420g/kWh) brake-specific fuel consumption (BSFC) and superior brake thermal efficiency of about 25.2 %. The emission results revealed that the DH20T blend showed the NO_X value increased by almost 10.97 % compared to diesel fuel, whereas the CO, UHC, and smoke values reduced by roughly 31.25, 28.34, and 42.35 %. The optimum fuel blend (DH20T) result is recommended for agricultural engine applications.

* Corresponding author.
E-mail addresses: venkidsec@gmail.com (V. Rathinavelu), arulroll7@gmail.com (A. Kulandaivel), dr.arvind@arkajainuniversity.ac.in (A.K. Pandey), socse.rahul@dbuu.ac.in (R. Bhatt), melvinvictordepoures@gmail.com (M.V. De Poures), ihossain.phd@outlook.com (I. Hossain), asifulhs.dr@hotmail.com (A.H. Seikh), iqbal.phd@outlook.com (A. Iqbal), murugan.ponnusamy@ju.edu.et (P. Murugan).

1. Introduction

Recently, many energy conservation technologies have been followed by the source of biomass wastes [1], which was gathered from industrial, household and agricultural waste [2]. Developing countries faced waste disposal problems and enabled the bio-refinery technique [3]. The growing population associated with energy demand, urbanization, fossil fuel, and industrial concern found the consequences of environmental pollution [4]. Most recently, biohydrogen was found to be significant in alternative energy for a high calorific value of 142 kJ/g [5], clean combustion [6], and limiting pollutants [7]. The hydrogen fuel was extracted from bio-wastes like sewage sludge [8], coal, sawdust, and microalgae [9] via pyrolysis [10], Multipurpose solar-driven [11] and integrated systems [12], gasification with high heating rate batch reactor [13], supercritical water gasification [14] techniques. Among the various techniques, hydrothermal gasification promises energy recovery from solid and water waste [15]. Adapting a supercritical batch reactor enhanced the gasification system's efficiency [16]. Jayaraman et al. [17] studied and produced hydrogen from microbial sludge and species of red algae via a co-hydrothermal gasification process under 300-400 °C at 60 min. They reported that 15:200 g/mL feedstock to solvent ratio and 2:1 sludge to algae ratio operated by 360 °C and found a maximum hydrogen yield of 36.1 %. Gong et al. [18] extracted the hydrogen from dewatered sludge through a supercritical water and hydrothermal gasification process under 60 min at 250 °C. They studied the behaviour of different catalysts on hydrogen yield, energy recovery & H_2 selectivity and found that the KOH catalyst offered maximum hydrogen yield compared to others. To maintain the environmental life cycle system, sewage wastewater has been subjected to various treatments to manage the energy savings from sewage sludge to biogas and avoid carbon dioxide emissions [19].

Moreover, recent research promotes the catalysts for hydrogen production due to their excellent performance compared to conventional methods [20]. In addition, the sewage sludge treated by hydrothermal gasification process promised hydrogen was utilized as an alternative fuel for minimized pollution degradation [21]. Bora et al. [22] reviewed and summarized the sustainable approach for gathering alternative fuel from sewage wastewater. It could be processed by obtaining the syngas utilized for engine application, which is found to be economical and efficient. They summarized the various fuel blends' actions on engine performance and emission characteristics. Besides, the microalgae have the potential for hydrogen production and are utilized for fundamental applications [23]. The compression ignition engine performance and emission behaviour were recently evaluated using hydrogen fuel from the waste sewage/microalgae. With the significance of hydrogen fuel, the system's thermal efficiency was hiked by 4.85 % with a higher calorific value, and the CO/HC emission was limited by 25 and 22.22 %, respectively [24]. Likewise, biofuel blend with diesel fuel with volume ratios of 10, 20, and 30& and their performance was measured by various loading conditions. The 10 vol% fuel blend results in better engine performance, and its emissions were reduced by 11 % on unburned carbon, 26 % on carbon dioxide, and 12 % on particles compared to others [25]. However, the green hydrogen gathered from bio-renewable sources is promising for future energy applications [26]. Applying an anaerobic digestion technique of sewage water was synthesized by bio-gas and green hydrogen for the future trend for several energy applications [27].

Moreover, the NOx was limited by 23.66 % on 220 bar pressure, with liquid fuel replacement at 85 %. In the last five decades, Adar et al. [28] studied the effect of gasification of sludge treated with a KOH catalyst operated at 540 °C under continuous reactor action; at 540 °C, the hydrogen molar proportion with KOH reached 60 %. However, the efficiency of the fuel blend was improved by additives, and TiO_2 was found to have higher performance, like good chemical stability, non-toxic, and economical compared to other additives [29]. This helps to increase the brake thermal efficiency and reduce the specific fuel consumption [30].

A lot of literature relevant to hydrothermal gasification, hydrogen fuel, green hydrogen gas production techniques and engine performance behaviour are summarized, and the gasification temperature and time to process is the main factor for deciding the hydrogen yield during the hydrothermal gasification process for waste sewage sludge and Algae. In this regard, the present research aims to synthesize the hydrogen from Algae gathered from sewage sludge waste through a hydrothermal gasification reaction associated with a KOH catalyst functioned by 6–30 min processing time along with 500-800°C gasification temperature. The optimum

Fig. 1. Open-type wastewater pond.

gasification time and temperature for gaining the maximum hydrogen yield with superior gasification efficiency are monitored. The obtained hydrogen gas was effectively utilized as an alternative fuel for internal combustion engines with different diesel/TiO_2 particle blends for agriculture engine applications. The effect of fuel blends on engine performance and emission was measured experimentally. The results showed enhanced engine performance with proven reduced engine emission compared to diesel fuel.

2. Materials and methods

2.1. Wastewater collection

Waste-activated sludge from water treatment plants is a relatively recent energy source for the manufacture of biofuels when compared to biomass generated from plants. These sewage sludges have several benefits, including a rapid growth rate with CO_2 fixation, the ability to cultivate microalgae during wastewater treatment, and the ease with which they may be utilized as a feedstock due to their high carbohydrate content and easy structure. The sewage sludge waste feedstock was collected and stored in open atmospheres like water ponds, as shown in Fig. 1. Initially, the properties of wastewater, like ammoniacal nitrogen, phosphate, and pH content, were measured, followed by filtering the wastewater with a mesh cloth to remove the floating debris. A mesh cloth size of about 35(m) was utilized, and the chemical oxygen demand (COD), ammoniacal nitrogen, and phosphate were measured using ascorbic acid [22].

2.2. Cultivation system

Several cultivation systems have been available for small- and large-scale algae production in recent years. Hence, the cultivation system is selected based on nutrient supply, algae spices, and the influence of the microalgae production technique used.

2.3. Sludge and algae production

A typical microbe isolation methodology soil near the sewage treatment facility extracts the microorganisms essential to sludge formation. The wastewater was inoculated with microbes to make microbial sludge. 1l of wastewater was supplemented with about 4500 cells, which were then oxygenated for 12 h at room temperature. The COD, ammoniacal nitrogen, and phosphate concentrations in the sludge were then measured after the sludge and effluent were separated by Whatman filters (15 mm pore size). In hydrothermal gasification tests, the sludge and the algae were used as the feedstock. Because of this, algae cells have chlorophyll, enabling them to photosynthesize by converting carbon dioxide into cellular material using sunlight photosynthesis. Algae development is improved to a certain extent during photosynthesis by increasing light intensity and lower light intensity decreases the algae production. Besides, light energy is offered to split the wastewater molecules like electrons, protons, and oxygen. By photophosphorylation, the molecular enhances the adenosine triphosphate with an improved oxygen nature. This photosynthesis effect of the sewage water process is mentioned in equation (1), which indicates the conversion of wastewater carbon dioxide and water into oxygen and glucose during the light energy.

$$6CO_2 + 6H_2 + light\ energy \rightarrow C_6H_{12}O_6 + 6O_2 \tag{1}$$
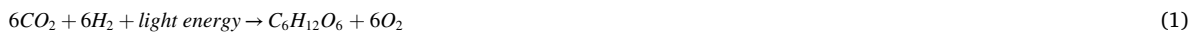
With the use of UV-Vi's spectrophotometry, the development of the algae was constantly observed. Before and during algae cultivation, phosphate, COD, and ammoniacal nitrogen contents were noted.

Moreover, algae's 100 % feedstock contains higher CO_2 [31]. Fig. 2 shows hydrothermal gasification using photosynthesis. The
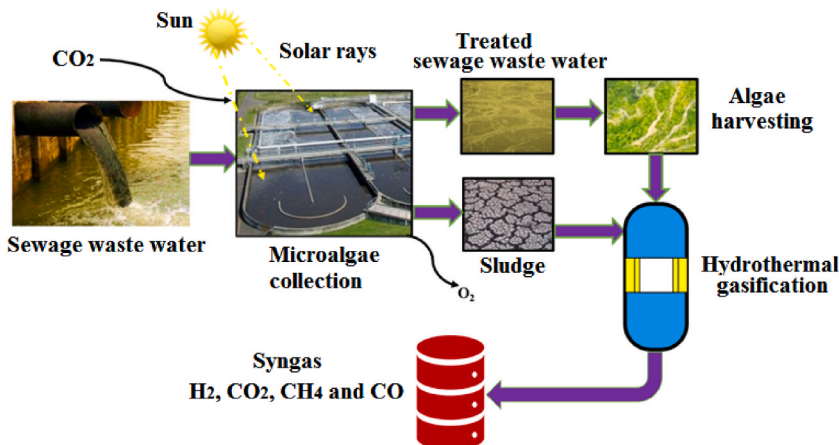

Fig. 2. Schematic diagram for the production of hydrogen from sewage sludge wastewater and Algae waste.

sewage wastewater/microalgae is initially collected and stored in open sunlight. It is involved in the photosynthesis process addressed above. The chemical makeup of algae biomass primarily includes proteins, carbohydrates, and lipids. Proteins comprise 50–70 % of dry biomass, followed by carbohydrates (30–40 %) and lipids (10–20 %). The treated sewage wastewater/Algae subjected to hydrothermal gasification reactions is detailed in section 2.4.

The proximate and ultimate analysis of algae and sewage sludge is shown in Table 1 [31,32]. The functional group and the structural characteristics of sludge and algae were analyzed by using FTIR spectra analysis. High water dispersibility indicates that an oxygen-containing functional category is present and algae have effectively oxidized. Fig. 3 shows the FTIR spectra analysis for sewage sludge and algae.

2.4. Hydrothermal gasification

During the hydrothermal gasification reaction (HGR), the algae were utilized as feedstock for the gasification process. HGR is a technique that changes algae biomass to syngas through processes of algae and sludge as organic waste. To create a synthesis gas, it utilizes water in the algae as the catalyst during its supercritical operation phase. The HGR have four standard operations for the production of syngas. These are the drying of algae and sludge, pyrolysis process, combustion in gasification, and reduction of CO_2. The gas chromatograph (Micro-9100) was utilized to measure syngas composition from the HGR. The combustion temperature was set to heat to 450 °C in equilibrium for 1 min, then to 520 °C at a rate of 70 °C/min, then to 640 °C at a rate of 120 °C/min, and kept at this temperature for 3 min [32]. The actual experimental setup for the hydrothermal gasification process is shown in Fig. 4.

This study used multiple operating conditions for the HGR to choose the best working conditions for higher hydrogen production. At first, different reactions were run for varying amounts of time at a constant reactor temperature of roughly 500 °C. Approximately 500–800 °C is the temperature range for HGR, and the reaction duration is about 6–30 min under 250 bar. Each experiment was performed three to four times, and the average value was used for the conversion efficiency calculations. Besides, the catalytic properties of ash may vary due to the feedstock content during the hydrothermal gasification process and sufficient alkali metals such as sodium and potassium, which enhances the gas conversion [33]. The activity of KOH catalytic facilitates enriching the overall efficiency of the gasification process and obtaining the higher conversion of hydrogen and methane gasses under maximum pressure and temperature. In addition, the cyclone separator helps to remove the solid particulate from the stream of syngas, and the incorporation of an alumina-silica membrane supports the separation of hydrogen from syngas. Here, the gas chromatograph (Micro-9100) was adapted to analyze the compositions of syngas gas gathered from HGR. This analytical control tool facilitates enumerating the effect of KOH and ash particulate distribution while measuring syngas gas yield. The uncertainty for the gas product was less than 2.52 %, and the uncertainties for pressure and temperature were less than 2.33 % and 2.62 %, respectively [34].

2.5. Data interpretation

H_2 selectivity, Carbon gasification efficiency (CE), Lower heating value (LHV), Hydrogen yield potential (HYP), and gasification efficiency (GE) were used to assess the impact on the hydrothermal gasification of sewage sludge and algae gas output. Equations (2)–(5) were used to determine the parameters mentioned above [31].

$$H_2 \text{ selectivity} = \frac{amount\ of\ hydrogen\ moles}{2 \times moles\ of\ methane} \tag{2}$$

$$CE = \frac{Total\ carbon\ in\ syngas}{Total\ carbon\ in\ feedstock} \tag{3}$$

$$LHV = (0.108 \times VH_2 + 0.126 \times VCO + 0.358 \times VCH_4) \tag{4}$$

$$GE = \frac{Quantity\ of\ all\ gas\ phase\ products}{100\%\ of\ the\ entire\ mass\ of\ sewage\ sludge\ and\ algae\ (on\ a\ dry\ basis).} \tag{5}$$

Where i stands for H_2, CO, and CH_4 and V_i is the volume per cent of each gas as a percentage.

2.6. Compression ignition (CI) engine operated by hydrogen fuel

Furthermore, the hydrogen produced from HGR was utilized as a blended fuel in an internal combustion engine. The experimental layout of the CI engine setup is shown in Fig. 4. The test was carried out using a single-cylinder combustion engine with a water-cooled

Table 1
Proximate and Ultimate analysis of feedstocks.

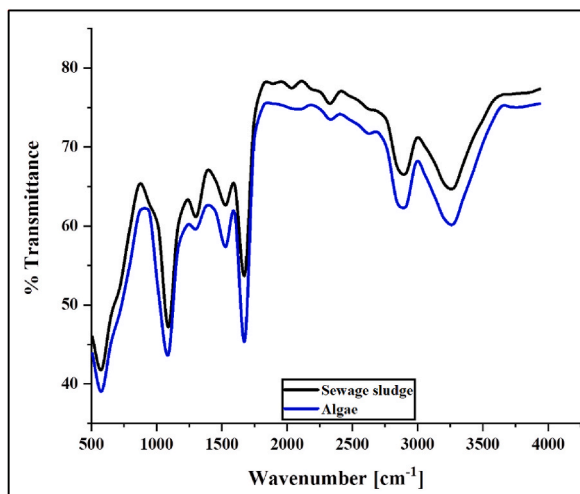| Feedstock	Proximate analysis				Ultimate analysis					LHV (MJ/kg)
	Volatile matter (%)	Fixed carbon (%)	Ash (%)	Moisture (%)	C	H	O	N	S	
Algae	66.4	23.2	11.2	80	42.5	6.7	30.2	7.1	1.9	15.23
Sewage sludge	61.6	9.4	27.56	74	38.18	3.4	24.56	4.98	1.05	14.63

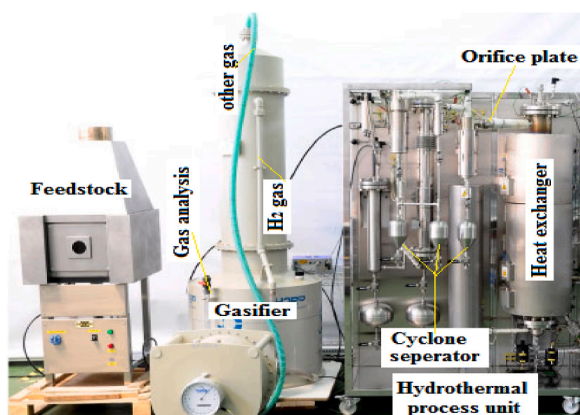**Fig. 3.** FTIR analysis of sewage sludge and algae.

Fig. 4. Hydrogen production from hydrothermal gasification.

system. A hydrogen fuel was added to the Simpson 217 engine's clean diesel as a secondary fuel. The schematic layout of the experimental setup for engine characteristics analysis is shown in Fig. 5. Two regulators have been included in the injector so that operators can regulate diesel and hydrogen flow rates from the storage tank. The electric unit controlled the fuel injector. The temperature inside the combustion chamber was measured using K- a type thermocouple. The dynamometer was connected to the engine
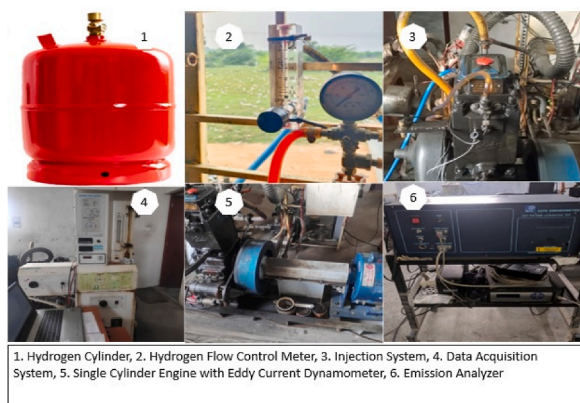

1. Hydrogen Cylinder, 2. Hydrogen Flow Control Meter, 3. Injection System, 4. Data Acquisition System, 5. Single Cylinder Engine with Eddy Current Dynamometer, 6. Emission Analyzer

Fig. 5. Experimental layout of the CI engine setup.

and the Data acquisition system was connected to the computer to collect and record the test data. The smoke opacity, also tied to the engine's exhaust system, was measured using the smoke meter (AVL 437C).

Furthermore, the fuel was mixed with hydrogen and Titanium Dioxide (TiO_2) to measure the effect of hydrogen and nanoparticles on engine performance. Hence, the engine was tested initially by using only diesel and then blended with hydrogen such as Diesel 100 % (D), Diesel 90 % and H_2 10 % (H10), Diesel 80 % and H_2 20 % (H20), Diesel 100 % and 100 ppm TiO_2 (DT), and Diesel 90 % and H_2 10 %, and 100 ppm TiO2 (DH10T), and Diesel 80 % and H_2 20 %, 100 ppm TiO_2 (DH20T). Table 2 shows the various blends for this investigation and the properties of these blends.

In general, handling hydrogen requires extreme caution because it ignites easily when oxygen is present. Hence, the engine combustion, performance, and emission characteristics like cylinder pressure, heat release rate (HRR), Brake thermal efficiency (BTE), brake specific fuel consumption (BSFC) were analyzed at various engine speeds of about 1600, 1800, 2000, 2200, 2400, 2600 rpm. Filters were used to increase the purity of the hydrogen supply.

Among the various additives, TiO_2 is non-toxic, has good chemical stability, and is low-cost [35]. Previous research proved the significance of TiO_2, which was (100 ppm) blended with diesel fuel, found 29.65 % improved brake thermal efficiency and reduced brake-specific fuel consumption by 5.16 % [36]. Based on this, TiO_2 was considered and blended with diesel fuel as 100 ppm.

3. Results and discussion

3.1. Effect of reaction time on molar fraction and LHV, gas yield and H_2 selectivity, CE, GE, and HYP of hydrothermal gasification process for sewage sludge and algae

Fig. 6 illustrates the effect of reaction time on a) Molar fraction and LHV, (b) Gas yield and H_2 selectivity, and (c) CE, GE, and HYP of hydrothermal gasification process for sewage sludge and algae. The reaction was one of the factors for deeding the hydrogen yield. It was observed from Fig. 6(a) that the molar fraction of H_2 gradually increased with increased time duration from 6 to 30 min under the interval of 6 min.

The 30 min reaction time showed the maximum H_2 molar fraction and showed 34 % improvement compared to the 6 min duration of reaction time. The improved hydrogen was due to the accumulation of gas being improved with increased time [37]. Meantime, carbon monoxide was significantly decreased with increased reaction time. It was due to the presence of a special type of membrane filter. Moreover, the system's lower heating value (LHV) will be reduced marginally on improved time duration. The LHV for a 30 min time duration showed 10.4MJ/Nm^3.

Fig. 6(b) represents the bar chart illustration of the effect of reaction time on H_2 sensitivity, H_2, CO, CO_2, and CH_4. It showed a progressive improvement in syngas with an increase in reaction time. The yield of H_2 gas was higher than that of CO, CO_2, and CH_4 gas. It proved the hydrogen yield improvement on every 6 min time gap and found a maximum yield of 26 mol/kg. Compared to the 6 min reaction time, it was hiked by 1.88 times. It was due to a biochemical reaction [18]. Moreover, H_2 sensitivity was linearly improved with improved reaction time from 6 to 30 min, and higher H2sensitivity (17.3) was found on 30 min reaction time.

Similarly, the GE, CE and HYP were increased with increased reaction duration from 6 to 30 min under the intervals of 6 min. The GE, CE and HYP values of about 56 %, 58 % and 69 mol/kg were recorded at higher reaction durations (30 min), as shown in Fig. 6(c). The increase in residency time was shown to cause only a slight modification in each conversion value, and the overall trend of change for each reaction duration was also found to be less.

However, time was a significant factor in improving the hydrogen gas yield, which was connected to H_2 sensitivity, GE, CE, and HYP. Based on the investigation, the hydrogen yield was improved by 1.88 times of 6 min duration and compared to past literature reported (360 °C at 60 min) by Jayaraman et al. [17], it was enhanced by 55.12 %. According to the present investigation result for hydrogen, the yield was compared to recent literature, shown in Table 3.

Table 3 shows the novelty of the current investigation compared to the recent literature report. The hydrogen yield increased by 32.9 % and 6.43 % compared to recent literature reported by Jayaraman et al. [17] and Gong et al. [18]. However, the temperature of the gasification process plays a prominent role in hydrogen yield.

3.2. Effect of temperature on molar fraction and LHV, gas yield and H_2 selectivity, CE, GE, and HYP of hydrothermal gasification process for sewage sludge and algae

Influences of temperature reaction time on a) Molar fraction and LHV, (b) Gas yield and H_2 selectivity, and (c) CE, GE, and HYP of hydrothermal gasification process for sewage sludge and algae are shown in Fig. 7.

Table 2
Properties of D, H10, and H20 blend properties.

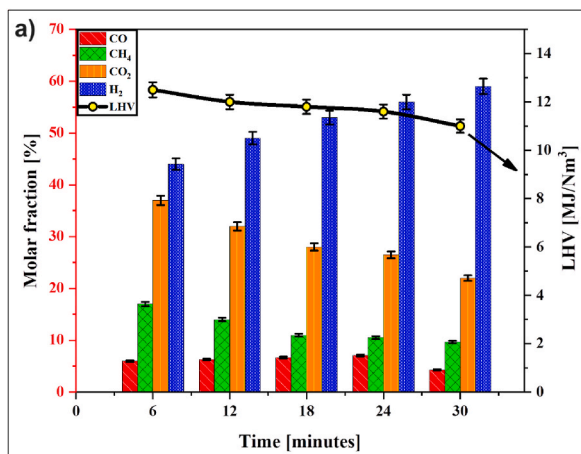| Properties	D	H10	H20	Test method
Density (kg/m^3)	820	875	845	ASTMD4052
Calorific Value (MJ/kg)	43200	39800	41500	ASTDM240
Kinematic Viscosity at 40 (mm^2/s)	3.05	5.6	4.3	ASTMD4052
Flash Point 0 °C	72	125	105	ASTMD93
Cetane Number	43.2	54	51	ASTMD613

Fig. 6(a). Effect of reaction time on Molar fraction (%) and LHV.
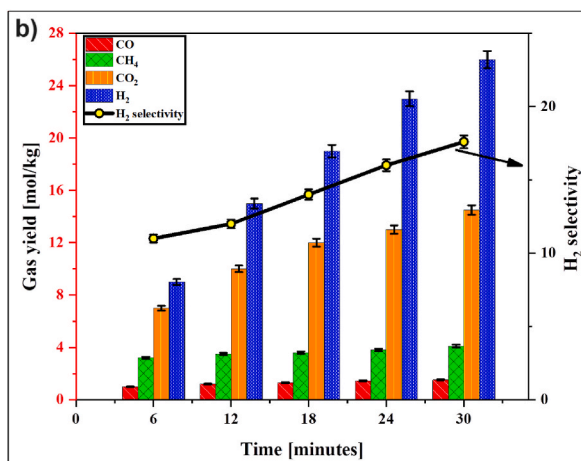

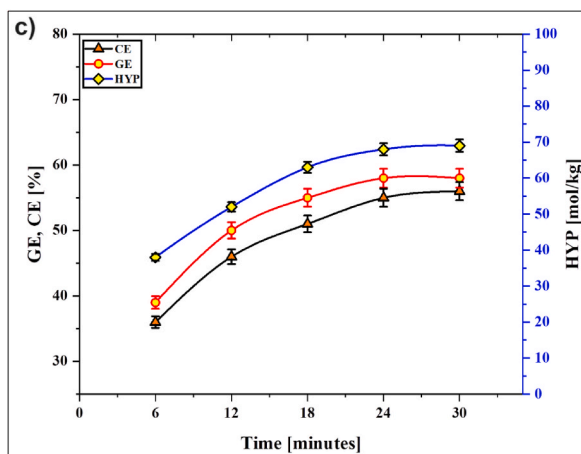**Fig. 6(b).** Effect of reaction time on Gas yield and H_2 selectivity.

Fig. 6(c). Effect of reaction time on CE, GE, and HYP.

Table 3
Comparison of hydrogen yield.

S. No	Source	Process	Temperature in °C	Time in minutes	H_2 Yield in %	Reference
1	Microbial sludge and algae	Co-hydrothermal gasification	360	60	36.1	[17]
2	Dewatered sludge	Supercritical Hydrothermal gasification	250	60	45.1	[18]
3	Sewage sludge and algae	Hydrothermal gasification with KOH catalyst	800	30	48	Present investigation

Fig. 7 (a) represents the effect of temperature on molar fraction and LHV of the hydrothermal gasification process for sewage sludge and algae. It was noted from Fig. 7 that the molar fraction of H_2 was inversely proportional to the CO, CO_2, and CH_4 gas at increased temperatures from 500 to 800 °C. During the steam process, the gasification system found a maximum yield of H_2 with reduced CO, CO_2, and CH_4 gas. The catalyst adopted a supercritical system to find an increased molar fraction of hydrogen rather than others [9, 13]. The maximum molar fraction of H_2 was 48 % at 800 °C and improved by 71.4 % compared to 500 °C. The experimental findings showed that increasing the gasification temperature improved the hydrothermal gasification of sewage sludge with algae from ionic degradation to free radical breakdown [15]. Hence, the LHV of algae decreased with an increase in the temperature of the gasification process. The highest LHV ($14MJ/Nm^3$) was recorded at a lower temperature of about 500 °C. As the gasification temperature increased, the mass fraction of liquid products steadily dropped.

The influences of gasification temperature on syngas yield and H_2 sensitivity of the hydrothermal gasification system are shown in Fig. 7 (b). The syngas yield was progressively improved with increased temperature of the gasification process, and the yield of H_2, CH_4, CO and CO_2 were 1.7, 4.4, 12.5, and 17.5 mol/kg at 800 °C. The increase in gasification temperature had a high biochemical reaction, resulting in a high H_2 yield [28]. It could imply that with higher temperatures, more significant amounts of carbohydrates in sewage sludge and algae breakdown [17]. In a similar trend, the sensitivity of H_2 significantly increased from 2.9 to 14.8 mol/kg with an improved temperature of 500 to 800 °C. High H_2 was due to carbonization reaction under higher gasification temperatures [18].

Fig. 7(c) represents the effect of gasification temperature on the hydrothermal gasification process's CE, GE, and HYP values on sewage sludge and algae. The CE, GE, and HYP values are about 45 %, 71 % and 54 mol/kg recorded at 800 °C temperatures, evidenced in Fig. 7 (c), which is the maximum value compared with other temperature ranges. The figure clearly shows that increases in gasification temperature increase the CE, GE, and HYP values with improved temperature values.

The abovementioned phenomenon showed that high temperature could significantly enhance hydrogen generation, which aligns with the calculated formula of H_2 selectivity with low LHV. Because three essential processes, such as pyrolysis, water gas shifting reaction, and steam reformation for producing H_2, were encouraged by increasing gasification temperatures, H_2 was accelerated [15–17].In these studies, as the gasification temperature rose, GE, CE, and HYP similarly improved. Based on the investigation report, the hydrothermal gasification process was executed for 30 min at 800 °C, found maximum hydrogen (H_2) yield, and was considered for further investigations. The sewage sludge and algae-derived hydrogen (H_2) were considered an alternative fuel and blended with different proportions on diesel & TiO_2 particles. The experimental measured CI engine performance is addressed below.

3.3. Effect of hydrogen and TiO_2 blend on CI engine performance

While the engine operated with H_2-rich syngas without purification, pretreatment is challenging for extended life and may vary due to the engine design, engine type, loading conditions, etc. [24]. Influences of H_2-rich syngas as the fuel without purification
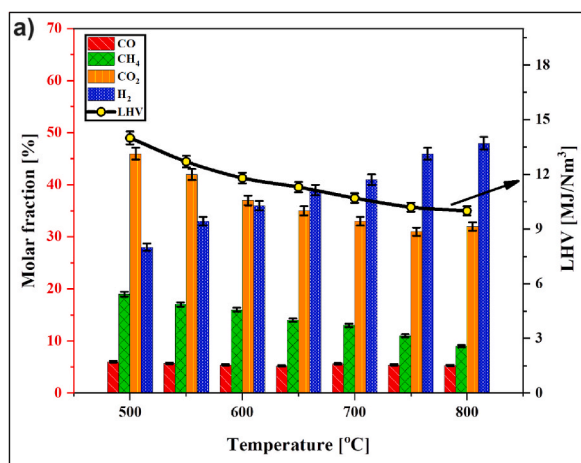

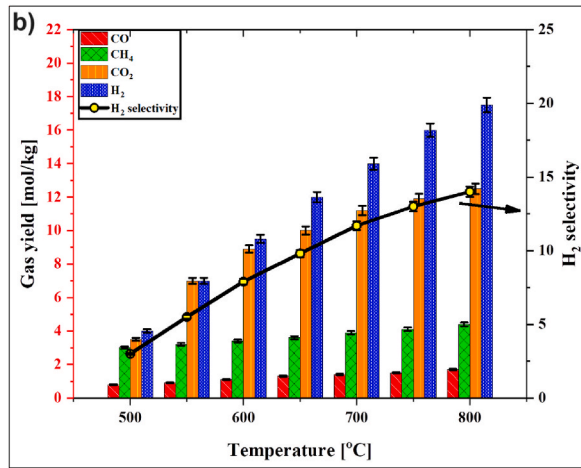**Fig. 7 (a).** Effect of temperature on Molar fraction (%).

Fig. 7 (b). Effect of temperature on Gas yield and H_2 selectivity.
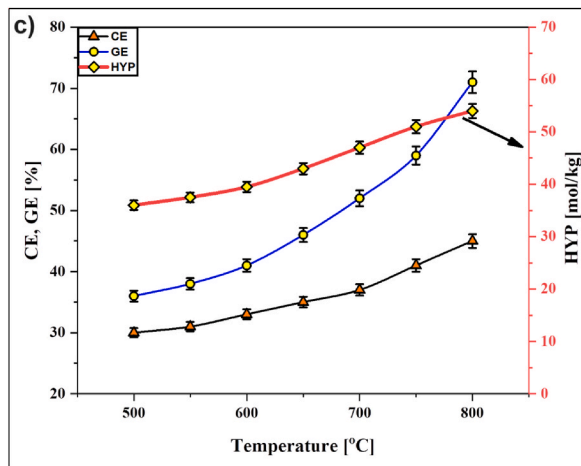

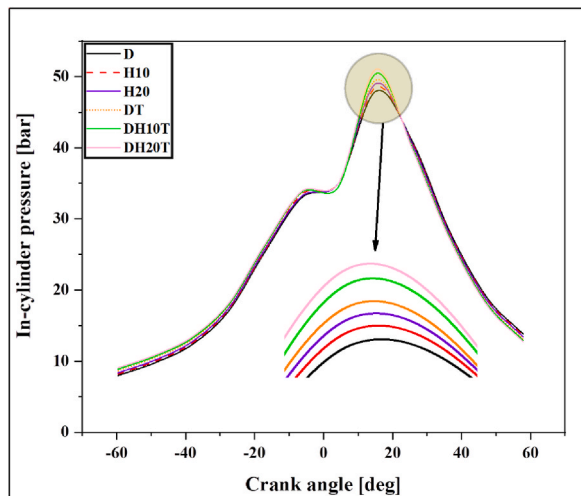**Fig. 7(c).** Effect of temperature on CE, GE, and HYP.

Fig. 8. In-cylinder pressure of the CI engine operates with different fuel blends.

pretreatment may cause losses of energy consumption [26]. So, the present investigation of hydrogen is pretreated by a catalyst process with the help of a cyclone separator to enhance the hydrogen gas quality and separate the particulate, and maximum hydrogen of 20 % is blended with diesel fuel spots for better engine performance and its results are addressed below.

3.3.1. In-cylinder pressure

Fig. 7 depicts the influences of hydrogen and TiO_2 blend with diesel fuel (D, H10, H20, DT, DH10T, and DH20T) behaviour on CI engine in-cylinder pressure measured with crank angle. Due to the enhancement of the desertification reaction, the TiO_2 is coupled with diesel fuel [26]. The reason for lower in-cylinder pressure was the chemical constitution of diesel fuel. Moreover, the in-cylinder pressure of the CI engine was increased gradually on different blends, and the DH20T blend facilitated a maximum in-cylinder pressure of 51 bar at a 15° crank angle. Due to this period, the hydrogen and diesel with TiO_2 were atomized in small spray particles, and the presence of TiO_2 limited the ignition delay. The pressure was increased by 6.47 % compared to diesel fuel without blending H_2 and TiO_2. It was higher than the other blends.

The higher in-cylinder pressure was due to the combinations of H_2 and TiO_2, which offered a clean and effective fuel mixture and increased pressure under the combustion stage. The in-cylinder was varied based on the blending ratio of diesel and biofuel [25]. Similarly, the in-cylinder pressure of other blends like D, H10, H20, DT and DH10T fuel was about 47.9, 48.5, 49, 49.7, and 50.4 bar, respectively. However, no ignition delay was found during the combustion process, and its in-cylinder pressure details are mentioned in Fig. 8.

3.3.2. Heat release rate (HRR)

The heat release rate (HRR) for the CI engine operated by various fuel blends is shown in Fig. 9. It was noted from Fig. 9 that the HRR of H_2 and TiO_2 blend with various volume percentages met the HRR peaks of diesel fuel and using the DH20T fuel blend in CI engine showed the higher HRR of 76J/°C recorded by 6° crank angle, which was the higher HRR compared with other fuel blends. It was due to the chemical properties of hydrogen fuel. Hydrogen has a higher calorific value [27]. Similarly, the CI engine operated with D, H10, H20, DT and DH10T fuel blend, showing the HRR was 65, 68, 71, 72, and 73.4J/°C, respectively. In CI engines, the first combustion stage is often when HRR reaches its most significant value. Low cetane fuels have a higher delayed ignition [24]. At the same time, the HRR of the DH20T fuel blend was compared with D (diesel) fuel, and a 16.92 % improvement was found.

Due to the DH20T blend's lower proportion of diesel and offering moderate viscosity and volatility, which improve fuel atomization and combustion, it has a greater HRR than other blends. Hence, the TiO_2 nanoparticles with hydrogen blends improve the combustion characteristics.

3.3.3. Brake-specific fuel consumption (BSFC)

The BSFC values for test fuel (D, H10, H20, DT, DH10T, and DH20T) are used to assess engine performance. These BSFCs were computed by using Equations (5)–(7) [24].

$$P_e = \frac{2\pi\omega\,T}{1000} \tag{6}$$

$$BSFC = \frac{m_f 10^3}{P_e} \cdot 100 \tag{7}$$

Where P_e is the power brake (kW), T is the torque (Nm), ω is the angular velocity, and m_f - is the fuel mass rate (kg/h).
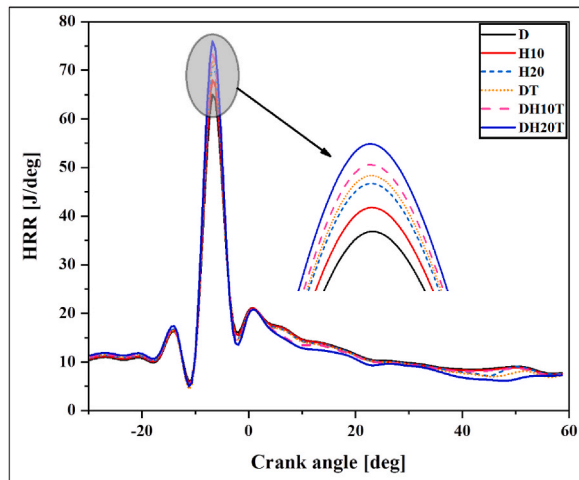

Fig. 9. HRR of the CI engine operates with different fuel blends.

The BSFC of CI engine operated with different fuel blends under 1600–2600 rpm engine speed is illustrated in Fig. 10. It was observed from Fig. 10 that the BSFC was progressively increased with an increase in the engine speed as 1600–2600 rpm and found the diesel blend with H_2, TiO_2, and combinations of H_2/TiO_2 showed gradual decreases in BSFC on increasing speed range. At the same time, the BSFC on diesel fuel and its different blends was noted as 402, 361, 322, 385, 341, and 302g/kWh at 1600 rpm, which was higher than the BSFC of the DH20T blend. The BSFC varied due to load, speed, and blending ratio, as reported by Aklouche et al. [25]. However, the DH20T blend was facilitated 420g/kWh on BSFC at a higher speed (2600 rpm) and was saved by 23.8 % compared to diesel fuel. As a result, the BSFC was even lowered at all speeds with the addition of TiO_2 nanoparticles with an increase in the proportion of hydrogen. The decrease in BSFC was made possible by the hydrogen and nanoparticle mixture's complete combustion and increased heating value.

3.3.4. Brake thermal efficiency (BTE)

The BTE was measured based on the function of BSFC and fuel heating value. The BTE for the CI engine was calculated by using Equation (7).

$$BTE = \frac{P_e 3600}{m_f LHV}.100 \tag{8}$$

The BTE values for all fuel blends D, H10, H20, DT, DH10T, and DH20T at various engine speeds of 1600, 1800, 2000, 2200, 2400, and 2600 rpm can be seen in Fig. 11. The central fact that can be concluded from Fig. 11 scatter graph was that the BTE was decreased with increased engine speed. The BTE value for using D, H10, H20, DT, DH10T, and DH20T fuel blends was about 22.5, 24, 25, 22.8, 24.3, and 25.2 % at 1600 rpm (lower engine speed). It's demonstrated that increasing engine speed decreases the BTE value of the engine. Similarly, the BTE value for using D, H10, H20, DT, DH10T, and DH20T fuel blends was about 15, 17.2, 18, 16, 17.5, and 19 % were recorded at higher engine speeds (2600 rpm). Adding biofuel blends with TiO2 nanoparticles gives a peak BTE value compared to non-nanoparticles. This is because the combination of nanoparticles and hydrogen produced a product with a decreased viscosity. The increased diffusivity and rapid speed of hydrogen flame cause the greater BTE [26]. Furthermore, complete combustion that increases BTE is prompted by a more excellent oxygen content and reduced viscosity. Moreover, the DT found higher Brake thermal efficiency compared to all others.

3.4. Effect of hydrogen and TiO_2 blend on CI engine emission performance

3.4.1. Carbon monoxide (CO)

Fig. 12 bar chart demonstrate the CO emission for CI engine operated by various fuel blends such as D, H10, H20, DT, DH10T, and DH20T at different engine speed of about 1600, 1800, 2000, 2200, 2400, and 2600 rpm respectively.

The CO emission of the engine using D, H10, H20, DT, DH10T, and DH20T was found to be 0.125, 0.093, 0.069, 0.12, 0.092, and 0.063 vol% at a higher engine speed of 2600 rpm and 0.083, 0.06, 0.041, 0.081, 0.055, 0.036 vol% were recorded by lower engine speed of 1600 rpm. In addition, the CO emission gradually increased with increasing engine speed. The higher hydrogen and TiO_2 nanoparticles content in the blended fuel could increase the availability of oxygen content in the fuel. A similar tendency was reported [24]. The biofuel's oxygen concentration, TiO_2 nanoparticles' reduction in viscosity, and the addition of hydrogen's greater diffusion rate and flame speed improve the clear combustion rate while leaving no unburned fuel behind. The unburned fuel components also cause more significant CO emissions from the engine.

Additionally, because hydrogen lacks carbon structure, less CO_2 is emitted. The TiO_2's large energy surface area was another justification for complete combustion. However, the CO emission of CI engines operated with DH20T was found to be the least emission and was limited by 49.6 % compared to diesel fuel-operated CI engines.

3.4.2. Unburned hydrocarbons (UHC)

Fig. 13: The bar chart represents the unburned hydrocarbon (UHC) of CI engine emission under different fuel blends at 1600–2600 rpm engine speed with an interval of 200 rpm.

Furthermore, the UHC represented as fuel only partially combusts in the combustion chamber, resulting in unfavourable engine performance. The UHC emission of engines using D, H10, H20, DT, DH10T, and DH20T was shown to be 252, 210, 172, 245, 202, and 160 ppm at 2600 rpm engine speeds. Similarly, the UHCs about 215, 167, 124, 219,149, and 113 ppm were recorded using the above fuel blend condition at a lower engine speed of 1600 rpm. It was shown that the UHC was increased gradually with increasing the engine speed, and the DH20T blend was found to reduce the level of UHC. It was lower than the value of other blends and diesel. Hence, the presence of H_2 and TiO_2 facilitates a clean mixture to clean-burning, offering completely burned fuel and finding the least amount of UHC. The hydrogen fuel blends with diesel fuel were found to have low UHC, as reported by Nithyanandhan et al. [24].

3.4.3. Nitrogen oxides (NO_X)

The NO_X emission of the engine by using various blends, such as D, H10, H20, DT, DH10T, and DH20T, at different engine speeds, as shown in Fig. 14. The NO_X emission of CI engines using D, H10, H20, DT, DH10T, and DH20T was about 241,368, 570, 230, 324 and 389 ppm were recorded at higher engine speeds.

. It was noted from Fig. 14 that the NOx emission gradually rose with increased engine speed and that D and DT had lower NOx emissions than all others. Higher NOx was due to hydrogen blends with diesel fuel, which was found to have a high calorific value,
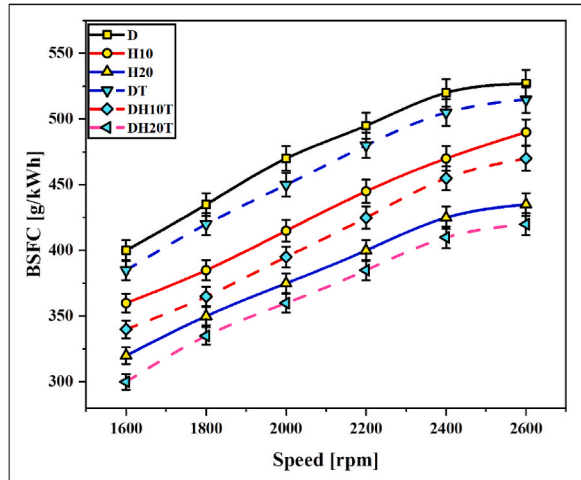
Fig. 10. BSFC of the CI engine operates with different fuel blends.
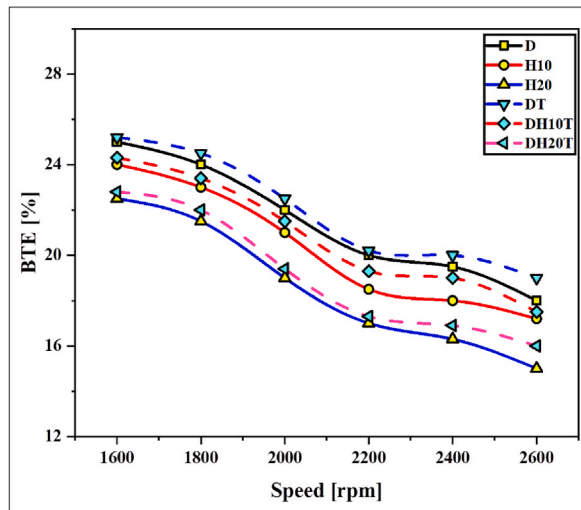

Fig. 11. BTE of the CI engine operates with different fuel blends.

resulting in increased heat value during the combustion. Similarly, higher cylinder temperature leads to NOx emission [27]. When NOx of non-nanoparticle fuel compared with fuel blended with nanoparticles could reduce the NOx emission of around 20-15 ppm. Due to its faster combustion rate than diesel, it was observed that adding hydrogen mixes to diesel caused the NOx to increase.

3.4.4. Smoke

Fig. 15 shows the smoke emission of the engine using D, H10, H20, DT, DH10T, and DH20T at different engine speeds 1600, 1800, 2000, 2200, 2400, and 2600 rpm. The smoke emission using D, H10, H20, DT, DH10T, and DH20T fuel blends was about 31, 22, 14.2, 27, 19.5, and 13 vol% recorded at higher engine speeds of 2600 rpm.

It was the maximum smoke emission value compared with other rates. The oxygen level in mixed gasoline and the addition of nanoparticles that break down the fuel for optimal complete combustion and reduce smoke emission may be to blame. The H_2 with TiO_2 nanoparticles for the engine also produces less smoke than diesel fuel without a blend. It results from the triple effect of homogeneous A/F mixture, the higher heating value of H_2, and more O_2 availability with an increasing catalytic activity that exhibits an enhanced premixed combustion phase [26]. Hence, the DH20T blend fuel gives the best engine performance result compared with other fuel blends.

4. Conclusion

Based on the investigation on hydrogen production by sewage sludge and algae wastewater effectively utilized to best convert it
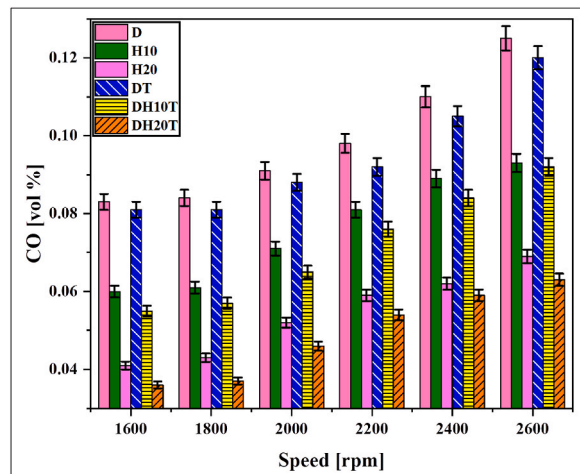
Fig. 12. CO emission of the CI engine operated by different blends.
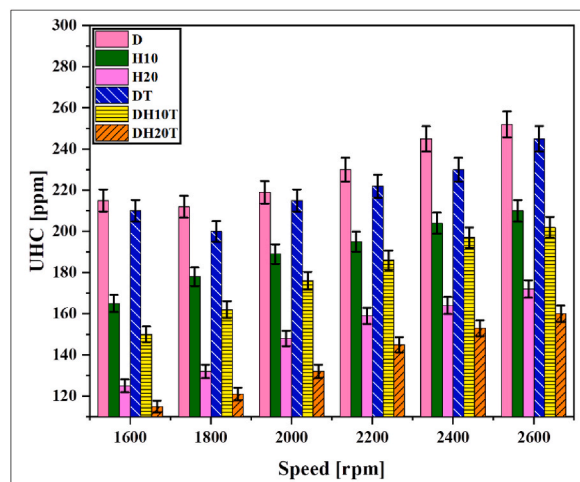

Fig. 13. UHC emission of the CI engine operated by different blends.

with hydrothermal gasification process with KOH catalyst, the maximum hydrogen yield was proven with different reaction times and temperatures. The key findings of the experimental results are summarized below.

- The gasifier operated at 800 °C temperature for 30 min found enhanced gas yield, such as a 71.4 % improvement in molar fraction %. LHV was saved by 4 % and 1.88 times improved H_2 yield compared to a 6 min reaction time under 500 °C temperature.
- Moreover, the GE (56 %), CE (58 %), and HYP (69 mol/kg) were found to have higher values than others. In addition, the produced H_2 from the hydrothermal gasification was further utilized in the IC engine as an alternative fuel.
- The H_2 blended with diesel and TiO_2 nanoparticles to vary the engine system's combustion, performance, and emission characteristics were studied, and it was observed that the DH20T blend was found to have superior engine performance.
- The in-cylinder was improved by 6.47 %, HRR raised to 16.92 %, the BSFC was saved by 23.8 %, and BTE improved by 12 % compared to diesel blends.
- Compared to diesel fuel, an IC engine fueled by a combination of hydrogen and TiO_2 nanoparticles has shown a minor improvement in performance and a sizable reduction in CO, UHC, NO_X, smoke, and emissions.
- In the future, hydrogen fuels are recommended as the prime source and fulfil the applications of alternative fuels for automotive. In addition, the yield of hydrogen fuel was improved by using a special type of reactor and optimizing the gasification process parameters.

Data availability

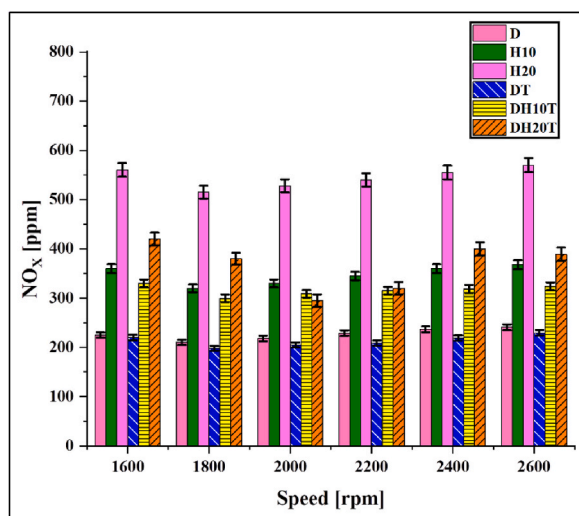All the data required are available within the manuscript.

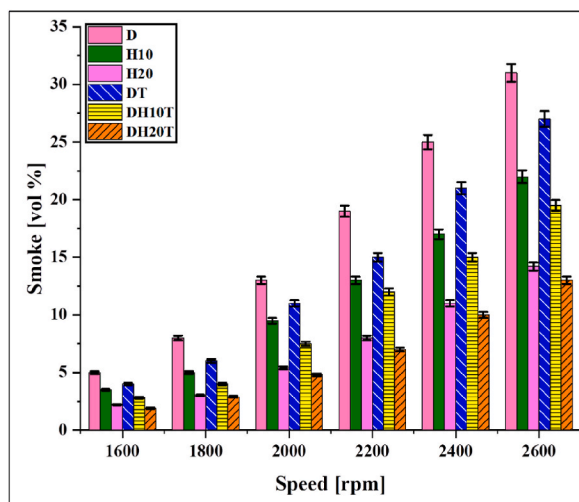**Fig. 14.** NO$_X$ emission of the CI engine operated by different blends.

Fig. 15. Smoke emission of the CI engine operated by different blends.

Additional information

No additional information is available for this paper.

CRediT authorship contribution statement

Venkatesh Rathinavelu: Data curation, Conceptualization. **Arul Kulandaivel:** Software, Resources. **Arvind Kumar Pandey:** Methodology, Investigation. **Rahul Bhatt:** Resources, Project administration. **Melvin Victor De Poures:** Supervision, Software. **Ismail Hossain:** Visualization, Validation. **Asiful Hossain Seikh:** Data curation, Conceptualization. **Amjad Iqbal:** Funding acquisition, Formal analysis. **P. Murugan:** Writing – review & editing, Writing – original draft.

Declaration of competing interest

The authors declare that they have no known competing financial interests or personal relationships that could have appeared to influence the work reported in this paper.

Acknowledgements

References

[1] W. Foster, U. Azimov, J. Munoz, Waste-to-energy conversion technologies in the UK: processes and barriers e a review, Renew. Sust. Energy. Rev. 135 (2021) 110226, https://doi.org/10.1016/j.rser.2020.110226.

[2] A. Jain, S. Sarsiya, J. Shi, Bioenergy and bio-products from bio-waste and its associated modern circular economy: current research trends, challenges, and future outlooks, Fuel 307 (2022) 121859, https://doi.org/10.1016/j.fuel.2021.121859.

[3] A.S. Nizami, M. Rehan, D. Pant, Waste biorefineries: enabling circular economies in developing countries, Bioresour. Technol. 241 (2017) 1101–1117, https://doi.org/10.1016/j.biortech.2017.05.097.

[4] Y. Ferrer, H. Perez, Los microorganismosen la digestion anaerobia y la produccion de biogas. Consideracionesen la eleccion del inoculo para elmejoramiento de la calidad y elrendimiento, ICIDCA Sobre Los Deriv La Cana Azúcar 43 (2010) 9–20.

[5] A. Mekonnen, S. Leta, K.N. Nju, Anaerobic treatment of tannery wastewater using ASBR for methane recovery and greenhouse gas emission mitigation, J. Water Process Eng. 19 (2017) 231–238, https://doi.org/10.1016/j.jwpe.2017.07.008.

[6] M.J. Park, J.H. Kim, D.W. Jeong, System optimization for effective hydrogen production via anaerobic digestion and biogas steam reforming, Int. J. Hydrogen Energy 45 (2020) 30188–30200, https://doi.org/10.1016/j.ijhydene.2020.08.027.

[7] L. Sillero, R. Solera, M. Perez, Anaerobic co-digestion of sewage sludge, wine vinasse and poultry manure for bio-hydrogen production, Int. J. Hydrog. 47 (2022) 3667–3678, https://doi.org/10.1016/j.ijhydene.2021.11.032.

[8] M. Wilk, A. Magdziarz, I. Okalp, Hydrothermal carbonization characteristics of sewage sludge and lignocellulosic biomass. A comparative study, Biomass Bioenergy 120 (2019) 166–175, https://doi.org/10.1016/j.biombioe.2018.11.016.

[9] C. Yang, S. Wang, C. Cui, Thermodynamic analysis of hydrogen production via supercritical water gasification of coal, sewage sludge, microalga, and sawdust, Int. J. Hydrog. 46 (2021) 18042–18050, https://doi.org/10.1016/j.ijhydene.2020.06.198.

[10] A. Li, H. Han, J. Xiang, A novel sludge pyrolysis and biomass gasification integrated method to enhance hydrogen-rich gas generation, Energy Conv. Manag. 254 (2022) 115205, https://doi.org/10.1016/j.enconman.2022.115205.

[11] R. Venkatesh, W. Christraj, Experimental investigation of Multipurpose solar heating system, J. Energy Eng. 141 (3) (2013), https://doi.org/10.1061/(ASCE)EY.1943-7897.00001.

[12] L. Onnwuemezie, M.M. Ardekhani, Integrated solar-driven hydrogen generation by pyrolysis and electrolysis coupled with carbon capture and Rankine cycle, Energy Conv. Manag. 277 (2023) 116641, https://doi.org/10.1016/j.enconman.2022.116641.

[13] Y. Chen, L. Yi, L. Guo, Hydrogen production by sewage sludge gasification in supercritical water with high heating rate batch reactor, Energy 238 (2022) 121740, https://doi.org/10.1016/j.energy.2021.121740.

[14] C. Cao, Y. Xie, H. Jin, Hydrogen production from supercritical water gasification of soda black liquor with various metal oxides, Renew. Energy 157 (2020) 24–32, https://doi.org/10.1016/j.renene.2020.04.143.

[15] C. He, C.L. Chen, J.Y. Wang, Hydrothermal gasification of sewage sludge and model compounds for renewable hydrogen production: a review, Renew. Sust. Energy. Rev. 39 (2014) 1127–1142, https://doi.org/10.1016/j.rser.2014.07.141.

[16] Y. Chen, L. Yi, L. Guo, Hydrogen production by sewage sludge gasification in supercritical water with high heating rate batch reactor, energy 238 (2021) 121740, https://doi.org/10.1016/j.energy.2021.121740. Part A.

[17] R.S. Jayaraman, K.P. Gopinath, A. Pugazhendhi, Co-hydrothermal gasification of microbial sludge and algae Kappaphycusalvarezii for bio-hydrogen production: study on aqueous phase reforming, Int. J. Hydrog. 46 (31) (2021) 16555–16564, https://doi.org/10.1016/j.ijhydene.2021.02.038.

[18] M. Gong, A. Feng, Fan Yujie, Coupling of hydrothermal pretreatment and supercritical water gasification of sewage sludge for hydrogen production, Int. J. Hydrog. 47 (41) (2022) 17914–17925, https://doi.org/10.1016/j.ijhydene.2022.03.283.

[19] P.Z. Georgali, A. Kylili, A.M. Papadopoulos, Compost versus biogas treatment of sewage sludge dilemma assessment using life cycle analysis, J. Clean. Prod. 350 (2022) 131490, https://doi.org/10.1016/j.jclepro.2022.131490.

[20] H. Su, M. Yan, S. Wang, Recent advances in supercritical water gasification of biowaste catalyzed by transition metal-based catalysts for hydrogen production, Renew. Sust. Energy. Rev. 154 (2022) 111831, https://doi.org/10.1016/j.rser.2021.111831.

[21] F. Hongyu, C. Jintao, Y. Mi, Sewage sludge treatment via hydrothermal carbonization combined with supercritical water gasification: fuel production and pollution degradation, Rene. Energy 210 (2023) 822–831, https://doi.org/10.1016/j.renene.2023.04.071.

[22] A.P. Bora, D.P. Gupta, K.S. Durbha, Sewage sludge to bio-fuel: a review on the sustainable approach of transforming sewage waste to alternative fuel, Fuel 259 (2020) 116262, https://doi.org/10.1016/j.fuel.2019.116262.

[23] NishitSavla, S. Anushka, P. Soumya, 17 - microbial hydrogen production: fundamentals to application, Microbes Environ. Microbes and Environments (2020) 343–365, https://doi.org/10.1016/B978-0-12-819001-2.00017-6.

[24] K. Nithyanandhan, R. Sivakumar, Experimental investigation on performance, combustion and emission characteristics of CI engine with on-site hydrogen generation, Mater. Today: Proc. 46 (11) (2021) 5469–5474, https://doi.org/10.1016/j.matpr.2020.09.199.

[25] F.Z. Aklouche, L. Hadhoum, M. Tazerout, A comprehensive study on effect of biofuel blending obtained from hydrothermal liquefaction of olive mill waste water in internal combustion engine, Energies 16 (6) (2023) 2534, https://doi.org/10.3390/en16062534.

[26] D. Banerjee, N. Kushwaha, E. Ahmad, Green hydrogen production via photo-reforming of bio-renewable resources, Renew. Sustain. Energy Rev. 167 (2022) 112827, https://doi.org/10.1016/j.rser.2022.112827.

[27] M.U.B. Khawer, S.R. Naqvi, A. Ali, M. Naqvi, Anaerobic digestion of sewage sludge for biogas & biohydrogen production: state-of-the-art trends and prospects, Fuel 329 (2022) 125416, https://doi.org/10.1016/j.fuel.2022.125416.

[28] E. Adar, M. Ince, M.S. Bilgili, Supercritical water gasification of sewage sludge by continuous flow tubular reactor: a pilot scale study, J. Chem. Eng. 391 (2020) 123499, https://doi.org/10.1016/j.cej.2019.123499.

[29] S. Vellaiyan, A. Subbiah, P. Chockalingam, Effect of Titanium dioxide nanoparticle as an additive on the working characteristics of biodiesel-water emulsion fuel blends, Energy Sources: Recovery Util. Environ. Eff. 43 (9) (2021) 1087–1099, https://doi.org/10.1080/15567036.2019.1634776.

[30] S. Uslu, S. Simsek, H. Simsek, SM modelling of different amounts of nano-TiO_2 supplementation to a diesel engine running with hemp seed oil biodiesel/diesel fuel blends, Energy 266 (2022) 126439, https://doi.org/10.1016/j.energy.2022.126439.

[31] E.W. Becker, Microalgae: Biotechnology and Microbiology, vol. 10, Cambridge University Press, Cambridge, 1994.

[32] E. Uggetti, B. Sialve, E. Trably, J.P. Steyer, Integrating microalgae production with anaerobic digestion: a biorefinery approach, Biofuels BioprodBiorefn 8 (4) (2014) 516–529, https://doi.org/10.1002/bbb.1469.

[33] R.J. Moffat, Describing the uncertainties in experimental results, Exp. Therm. Fluid Sci. 1 (1) (1988) 3–17, https://doi.org/10.1016/0894-1777(88)90043-X.

[34] S. Siva Chandran, 'Magnesium alloy machining and its methodology: a systematic review and analyses, AIP Conf. Proc. 2473 (1) (2022), https://doi.org/10.1063/5.0096398(5.

[35] J. Isaac Premkumar, A. Prabhu, V. Vijayan, Combustion analysis of biodiesel blends with different piston geometries, J. Therm. Anal. Calorim. 142 (2020) 1457–1467.

[36] C. Dineshbabu, R. Venkatesh, Investigation of aspect ratio and friction on barrelling in billets of aluminium upset forging, Mater. Today Proc. 21 (1) (2019) 601–611.

[37] A. Mohana Krishnan, M. Dineshkumar, Evaluation of mechanical strength of the stir casted aluminium Metal matrix composites (AMMCs) using Taguchi method, 2022, Mater. Today Proc. 62 (4) (2022) 1943–1946.